Calibration Changes to Terra MODIS Collection-5 Radiances for CERES Edition 4 Cloud Retrievals

Sunny Sun-Mack, Patrick Minnis, Yan Chen, David R. Doelling, Benjamin R. Scarino, Conor O. Haney, and William L. Smith, Jr.

***Abstract*— Previous research has revealed inconsistencies between the Collection 5 (C5) calibrations of certain channels common to the Terra and Aqua Moderate Resolution Imaging Spectroradiometers (MODISs). To achieve consistency between the Terra and Aqua MODIS radiances used in the Clouds and the Earth's Radiant Energy System (CERES) Edition 4 (Ed4) cloud property retrieval system, adjustments were developed and applied to the Terra C5 calibrations for channels 1–5, 7, 20, and 26. These calibration corrections, developed independently of those used for the later MODIS Collection 6 (C6), ranged from −3.0% for channel 5 to +4.3% for channel 26. For channel 20, the Terra C5 brightness temperatures were decreased nonlinearly by 0.55 K at 300–10 K or more at 220 K. The corrections were applied to the Terra C5 data for CERES Ed4 and resulted in Terra–Aqua radiance consistency that is as good as or better than that of the C6 data sets. The C5 adjustments led to more consistent Aqua and Terra cloud property retrievals than seen in the previous CERES edition. After Ed4 began processing, other calibration artifacts were found in some corrected channels and in some of the uncorrected thermal channels. Because no corrections were developed or applied for those artifacts, some anomalies or false trends could have been introduced into the Ed4 cloud property record. Thus, despite the much improved consistency achieved for the Terra and Aqua data sets in Ed4, the CERES Ed4 cloud property data sets should be used cautiously for cloud trend studies due to those remaining calibration artifacts.**

***Index Terms*— Calibration, climate, cloud, Clouds and the Earth's Radiant Energy System (CERES), Moderate Resolution Imaging Spectroradiometer (MODIS).**

I. Introduction

THE NASA Clouds and the Earth's Radiant Energy System (CERES) is monitoring the earth's radiation budget and relies on broadband radiances measured by scanners on multiple satellites that are interpreted with the aid of high spatial resolution, narrowband spectral radiances taken simultaneously by imagers on the same satellites. The imager data are used to identify the scene as clear or cloudy and to estimate the relevant parameters necessary to characterize the scene, such as surface skin temperature or cloud optical depth (COD). These are used to select the appropriate broadband unfiltering procedure and angular directional models for converting the CERES instantaneous unfiltered radiances to outgoing top-of-atmosphere fluxes, to choose the proper directional or diurnal model for estimating the fluxes over the other hours of the day in order to compute daily averaged fluxes, and to calculate from the cloud properties the surface and atmospheric fluxes [1]. By themselves, the cloud properties comprise a climate data record (see [2]–[4]) and are valuable for evaluating climate models (see [5]–[7]). To construct reliable climate data records from the CERES measurements, it is critical not only to accurately calibrate the CERES broadband scanners but also to ensure that the imager calibrations are stable and consistent among the various platforms. Otherwise, calibration-dependent trends or differences can be introduced and produce artifacts in the climate record.

CERES uses the Moderate Resolution Imaging Spectroradiometer (MODIS) to retrieve cloud properties for the broadband scanners on the Terra and Aqua Sun-synchronous satellites. The MODIS calibration procedures are periodically updated to account for instrument degradation and new information that together improve the calibrations in the level-1B (L1B) data, which are reprocessed for each collection. Although the MODIS Collection 5 (C5) calibrations have been well characterized and carefully monitored for both Terra and Aqua [8]–[11], various researchers (see [9], [12]–[14]) determined that, in certain channels, there are some significant differences between the radiances measured by the Terra and Aqua MODIS copies, as well as degradation in some channels that were not reflected in the calibration L1B lookup tables used to convert counts to physical units. Such discrepancies can introduce significant differences in certain cloud properties retrieved from Terra and Aqua MODIS data (see [15], [16]) that could bias the CERES fluxes from Aqua relative to Terra. Furthermore, those differences could introduce spurious trends in the cloud properties from Aqua relative to their Terra counterparts. Thus, normalization of the imager calibrations, one to the other, is an essential part of the CERES processing system.

That system was designed to analyze the CERES data in sequence using, to the extent possible, consistent input data, algorithms, and calibrations over the entire CERES record.

Manuscript received December 21, 2017; revised March 15, 2018; accepted April 9, 2018. Date of publication May 18, 2018; date of current version September 25, 2018. This work was supported by the Clouds and the Earth's Radiant Energy System Project through the NASA Science Mission Directorate. *(Corresponding author: Sunny Sun-Mack.)*

S. Sun-Mack, P. Minnis, Y. Chen, B. R. Scarino, and C. O. Haney are with Science Systems and Applications, Inc., Hampton, VA 23666 USA (e-mail: szedung.sun-mack-1@nasa.gov).

D. R. Doelling and W. L. Smith, Jr. are with Science Directorate, Langley Research Center, National Aeronautics and Space Administration, Hampton, VA 23681 USA.

Color versions of one or more of the figures in this paper are available online at http://ieeexplore.ieee.org.

Digital Object Identifier 10.1109/TGRS.2018.2829902

TABLE I
MODIS CHANNELS USED IN CERES PROCESSING

MODIS Channel #	Central Wavelength (μm)	Ed2	Ed4	Name
1	0.65	Cloud mask, retrieval	Cloud mask, retrieval	VIS
2	0.86	--	Cloud mask	
3	0.47	--	Cloud mask	
4	0.55		TBD	
5	1.24	--	Cloud mask, retrieval	SNI
6	1.61	Cloud mask, retrieval (Terra)	--	
7	2.13	Cloud mask, retrieval (Aqua)	Cloud mask, retrieval	NIR
20	3.78	Cloud mask, retrieval	Cloud mask, retrieval	SIR
26	1.38	Cloud mask	Cloud mask	
27	6.71	Cloud mask	Cloud mask	WV
29	8.55	Cloud mask	Cloud mask	IRP
31	11.0	Cloud mask, retrieval	Cloud mask, retrieval	IRW
32	12.0	Cloud mask, retrieval	Cloud mask, retrieval	SWC
33	13.3	--	Cloud mask, retrieval	CO2

When the identification of programming errors, algorithm developments, and input and calibration improvements in one or more CERES subsystems have matured to a point sufficient to increase the accuracy of the CERES radiation record, they are incorporated into a revised system, and the CERES data are reprocessed over the length of record. Each version of the processing system for a given satellite is identified as an edition. To date, CERES has produced four editions for Terra and Aqua. Of those, only two have distinct cloud property processing streams, Edition 2 (Ed2) and Edition 4 (Ed4).

For lack of better information and having full confidence in onboard MODIS calibration systems, the Ed2 processing assumed that the Terra and Aqua calibrations were consistent. Hence, no adjustments were made to the radiances in the MODIS L1B data sets. The CERES Ed2 cloud mask and retrievals [13], [17] employed in the generation of CERES Ed2 and Edition 3 flux products used the MODIS Collection 4 (C4) data through 2007 and C5 data thereafter. No significant differences were found in the calibrations of the various channels between the C4 and C5 versions. Thus, the C5 Terra–Aqua (T–A) differences and the Aqua degradation noted earlier apply to the entire CERES Ed2 record and affect the CERES Ed2 cloud properties.

To account for the relevant calibration issues known at the time, the CERES cloud team independently developed methods to normalize the C5 radiances from selected Terra MODIS channels to their Aqua counterparts for the Ed4 processing. Concurrently, they formulated the CERES Ed4 cloud (see [19]) and flux algorithms to use the normalized C5 radiances. The Aqua channels were found to be very stable through 2008 [11], [12], [20]. Hence, the Aqua MODIS solar channels were selected to serve as the solar reflectance references for the Global Satellite Inter-Calibration System [21]. For the same reason, the Aqua channels were also selected as references used to adjust the Terra calibrations for CERES Ed4 processing. Implementation of the CERES Ed4 processing began in 2012, coincident with the initial release of the MODIS Collection 6 (C6) L1B radiances [18]. The C6 radiance calibrations represent an improvement over their C5 counterparts as they account for the Terra MODIS degradation and other newly found dependencies in some of the instrument's components [14], [18]. Because of the consistency constraints of CERES editions, Ed4 necessarily used C5 radiances until February 2017 when the production of C5 products ceased, Similar to the Ed2 case, which used two different collections, continuation of the Ed4 processing beyond January 2017 necessitates the utilization of C6 data, which may need to be adjusted to be consistent with the normalized C5 data.

This paper has multiple goals. First, it documents the development of the normalizations applied to the Terra C5 data used in CERES Ed4 and determines some of the effects of the calibrations on the CERES cloud property record. The adjusted C5 data are also compared with the C6 radiances to determine if they are consistent with each other and to provide the basis for adjusting the C6 data for use in Ed4 past January 2017. In Addition, calibration issues in other channels employed in the CERES algorithms, but discovered after Ed4 processing began, are examined and their potential impacts on the CERES cloud record are discussed. Knowledge of these remaining issues is critical for any future CERES editions.

II. DATA AND METHODOLOGY

A. Satellite Data

The CERES project receives a subsampled version of the full MOD02 (Terra) and MYD02 (Aqua) MODIS L1B calibrated geolocation data set. Data from every other pixel and scan line are provided for 19 out of 36 channels. Of those channels, only 12 are used in the cloud analysis, including seven solar reflectances and five infrared bands. The C5 L1B lookup tables are used to convert the counts to reflectance R for the solar reflectance channels and to radiance for the thermal emissive channels. Brightness temperature T is derived from the thermal radiances using the Plank function applied at the central wavelength of a given channel. Table I lists the channels and their use in the CERES processing system. Channel 4 is currently unused in the cloud analysis but is kept in the processing flow for possible use in later editions. The Aqua

1.6-μm channel was found to be too noisy and unreliable for use by CERES since the majority of the detectors are inoperable [20]. Thus, for consistency, no 1.6-μm data are used for either satellite in CERES Ed4 cloud processing. Instead, the 1.24- and 2.13-μm channels are used for cloud detection and secondary cloud particle size retrievals during processing of both the Aqua and Terra data [19].

For CERES Ed4, the solar channel data from July 2002 to December 2011 are used to normalize Terra channels to their Aqua counterparts throughout the Ed4 record, which continues as of this writing. Determination of calibration changes after 2011, however, was not continued because of processing constraints. To evaluate the calibrations, C6 L1B data are used for comparisons with the adjusted Terra C5 reflectances and brightness temperatures.

B. Solar Channel Normalizations

To effect the solar channel normalizations, the Terra and Aqua MODIS data were ray matched in the same manner used in [22]. The Terra and Aqua reflectances were matched both at nadir and off-nadir whenever they were taken within the same 15-min window, had the same viewing zenith angles, and the differences between their relative azimuth angles are less than 7.5°. The matched reflectances were averaged over the same 50-km region. No corrections were made for the minor spectral response function differences between the Terra and Aqua bands. Three periods were selected for normalization based on known artifacts in the Terra C5 data. Those artifacts are two sudden changes in the Terra calibration lookup tables that occurred on November 19, 2003 [12] and March 31, 2009 as a result of leaving the solar diffuser door open. The three periods extend from the launch of Aqua, May12, 2002–November 18, 2003; November 19, 2003–March 30, 2009; and March 31, 2009 to the end of the C5 record in 2017. The corrections developed for the final period are based only on the data taken between April 2009 and March 2011. Through an oversight, no changes were developed or applied prior to May 14, 2002.

The matched Terra and Aqua MODIS data, matched in the manner noted earlier, were used in linear regression as in [8] and [22], to compute force-fit slopes for each month within the three periods. Matches from 6 to 7 months in a given year had a sufficient number of matches to compute a slope [12]. Then, for each period, the correction factor, f_g, is estimated as

$$f_g = a_0 + a_1 * \mathrm{DSL} \tag{1}$$

and DSL is the number of days since the launch of Aqua, May 14, 2002. The coefficients, a_0 and a_1, were determined through least-squares linear regression based on the slopes computed for each month of the matched Terra and Aqua data within each interval. A value of a_1 was retained only if the slope was statistically significant.

The reflectances provided in the Terra MODIS C5 data set were altered for the three different periods by multiplying the nominal C5 reflectance, ρ_{C5}, by the correction factor in (1) to obtain the adjusted reflectance

$$\rho_{\mathrm{C5}'} = f_g * \rho_{\mathrm{C5}}. \tag{2}$$

The corrected Terra C5 data are hereafter denoted as C5' data.

The calibration changes are evaluated here by comparing the matched Terra and Aqua data from days 1, 11, and 21 from each month for 2003, 2008, 2013, 2015, and 2016 to sample segments of each calibration period with a special focus on more recent years to detect any degradation. For these comparisons, the Aqua and Terra data were matched using only those data taken within ±30 min and ±10° of solar zenith angle (SZA), and in the same 10° and 30° viewing zenith and relative azimuth angle bins, respectively. While these constraints are much looser than those used in [22], they provide a much greater amount of data. The matched data sets include both the original C5 and C5' data as well as the Terra MODIS C6 data. The Aqua C6 reflectances are negligibly different from their C5 counterparts, so that the Aqua C5 and C6 data are interchangeable. The magnitudes of the changes to Terra in C6 are variable with time and spectral band, and are significant in some instances.

C. Infrared Channel Normalizations

1) Channel 20, SIR (3.78 μm): Comparisons with Aqua MODIS between July 2002 and July 2005 show that the Terra MODIS measures SIR temperatures T_{Te} almost 0.55 K greater than Aqua during the daytime [13]. Thus, 0.55 K is subtracted during the daytime. During the night, T_{Te} can be from 1 to 3 K warmer than the Aqua temperature T_{Aq} when $T_{\mathrm{Te}} \sim 270$ K and up to 15 K warmer at $T_{\mathrm{Te}} \sim 220$ K. The example in Fig. 1 shows a scatterplot of Aqua and Terra SIR temperatures for July 2007 [Fig. 1(a)] and the corresponding temperature differences between Aqua and Terra, $T_{\mathrm{Aq}} - T_{\mathrm{Te}}$, as a function of T_{Te}. Such large differences between Aqua and Terra, especially at the low end, are seen in all MODIS C5 data records during nighttime. The nonlinearity in cold-end differences follows from the strong nonlinearity between temperature and radiance in the Planck function at this wavelength for the lowest temperatures in the troposphere.

Seasonal Terra SIR calibration curves [red line in Fig. 1(b)] were developed for each year by fitting values of $T_{\mathrm{Aq}} - T_{\mathrm{Te}}$ to a Gaussian error function (erf) as a function T_{Te}. The formula used is

$$T_{\mathrm{Aq}} = a_0 + a_1 * (\mathrm{erf}(a_2 * (T_{\mathrm{Te}} - 209.25)) + a_3 * (T_{\mathrm{Te}} - 209.25) \tag{3}$$

where the fitting coefficients a_i were computed using the matched data sets for each season for each year between July 2002 and August 2011. For application to the Terra data, a lookup table of $T_{\mathrm{Aq}} - T_{\mathrm{Te}}$ values, correction addends ΔT (C5'), was computed from the results of fitting (3) for each month in the center of each season at a resolution of 1.0 and 0.5 K for $T_{\mathrm{Te}} < 235$ K and $T_{\mathrm{Te}} > 235$ K, respectively. Lookup tables for each remaining month between June 2002 and July 2011 were created by linear interpolation between the seasonal center months. For the Terra data taken earlier than June 2002, the correction factors for

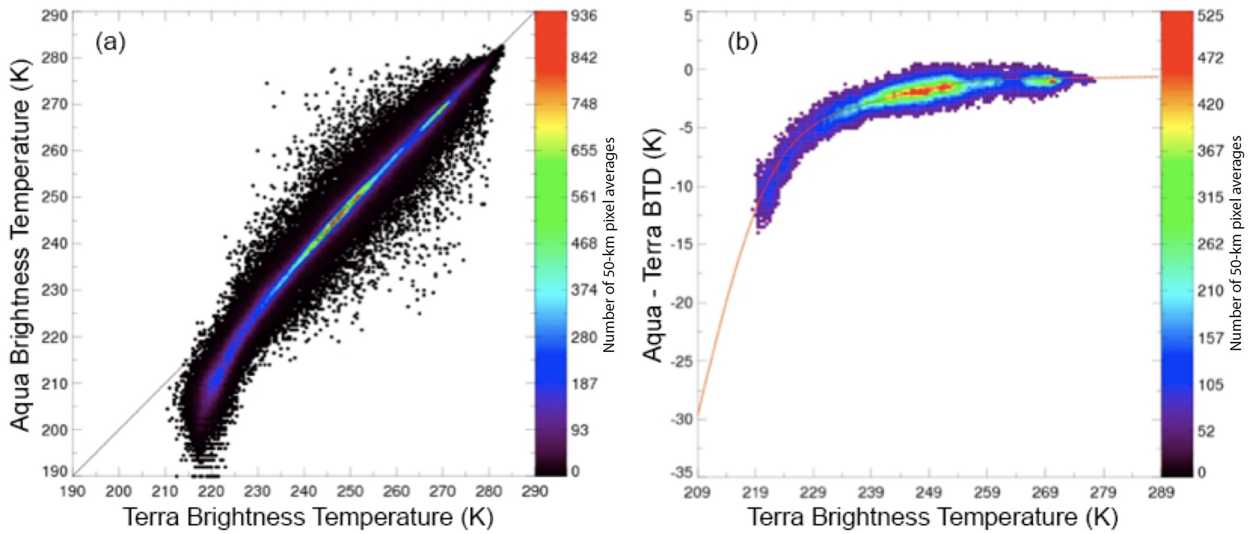

Fig. 1. Scatterplots of (a) Aqua and Terra C5 SIR temperatures for July 2007 and (b) corresponding SIR temperature difference between Aqua and Terra as a function of Terra SIR temperatures. Red line: Terra 3.8-μm nighttime calibration curve for July 2007.

TABLE II
CERES CALIBRATION COEFFICIENTS FOR (2) FOR TERRA MODIS C5 ED4 REFLECTANCES/RADIANCES

Channel	14 May 2002 -18 Nov 2003		19 Nov 2003 – 31 March 2009		After 31 March 2009	
	a_0	a_1	a_0	a_1	a_0	a_1
1 (0.65 µm)	1.0100	0.0	1.0190	0.0	1.0320	0.0
2 (0.87 µm)	0.9996	0.0	1.0010	2.904×10^{-6}	1.0059	0.0
3 (0.47 µm)	0.9958	1.182×10^{-5}	0.9997	9.662×10^{-6}	1.0368	0.0
4 (0.55 µm)	1.0016	0.0	1.0105	0.0	1.0219	0.0
5 (1.24 µm)	0.9724	0.0	0.9736	0.0	0.9706	0.0
7 (2.13 µm)	0.9927	0.0	0.9957	0.0	0.9995	0.0
26 (1.38 µm)	1.0307	0.0	1.0429	0.0	1.0430	0.0

July 2002–June 2003 are used for the relevant month. Likewise, lookup tables for July 2010–August 2011 are used for the Terra data taken after August 31, 2011. The typical uncertainty in the results of these fits is 0.0 ± 1.9 K. Much of the random error is likely due to the relaxed space and time constraints in matching the Terra and Aqua data.

In practice, the C5' values for Terra channel 20 were computed as follows. If the SZA $< 82.0°$

$$T_{\mathrm{Te}}(\mathrm{C5}') = T_{\mathrm{Te}}(\mathrm{C5}) - 0.55 \text{ K}. \tag{4}$$

Otherwise

$$T_{\mathrm{Te}}(\mathrm{C5}') = T_{\mathrm{Te}}(\mathrm{C5}) + \Delta T(\mathrm{C5}') \tag{5}$$

where the correction factor comes from the appropriate data month lookup table. These corrections are validated using the same matched Terra and Aqua data used to evaluate the solar channel calibrations.

2) Longwave Infrared Channels: Li *et al.* [23] found that the Terra and Aqua MODIS C5 infrared (10.8 μm), split window (SWC, 12.0 μm), and CO2 (13.3 μm) channels are consistent to ±0.1 K through 2012. No differences between daytime and nighttime were reported. No calibration changes were made to Terra for either of these channels. Terra and Aqua channels 27 (6.7 μm) and 29 (8.55 μm) C5 temperatures differ by 1.0 ± 0.9 K and 1.1 ± 0.7 K, respectively [23]. As these differences were unknown prior to the development of the Ed4 processing, no changes were made to the Terra calibrations for these channels. Any other differences found between the various channels are noted in the following sections. Comparisons between the Terra and Aqua MODIS longwave infrared channels for C5 and C6 data are performed here using the approach of [22].

III. COMPARISON OF TERRA AND AQUA CALIBRATIONS

Results are presented for the Terra channels that were adjusted. They are compared with their Aqua C5 counterparts as well as the corresponding Terra C6 data. Because the Aqua C5 and C6 calibrations are so similar, the comparisons of Terra with Aqua C5 would be the same comparing with Aqua C6.

A. Solar Channels

The calibration adjustment coefficients a_0 and a_1 applied to (1) are listed in Table II for seven Terra MODIS channels. The adjustment factor f_g is dominated by the first term in (2) of Section II-B; nonzero values for a_1 occur for only a few cases. Values for f_g range from 0.9706 for channel 5 to 1.043 for channel 26. Very small changes, <1%, are applied to the channels 2 and 7 C5 calibrations. For the most heavily used solar band in the Ed4 daytime algorithms, channel 1

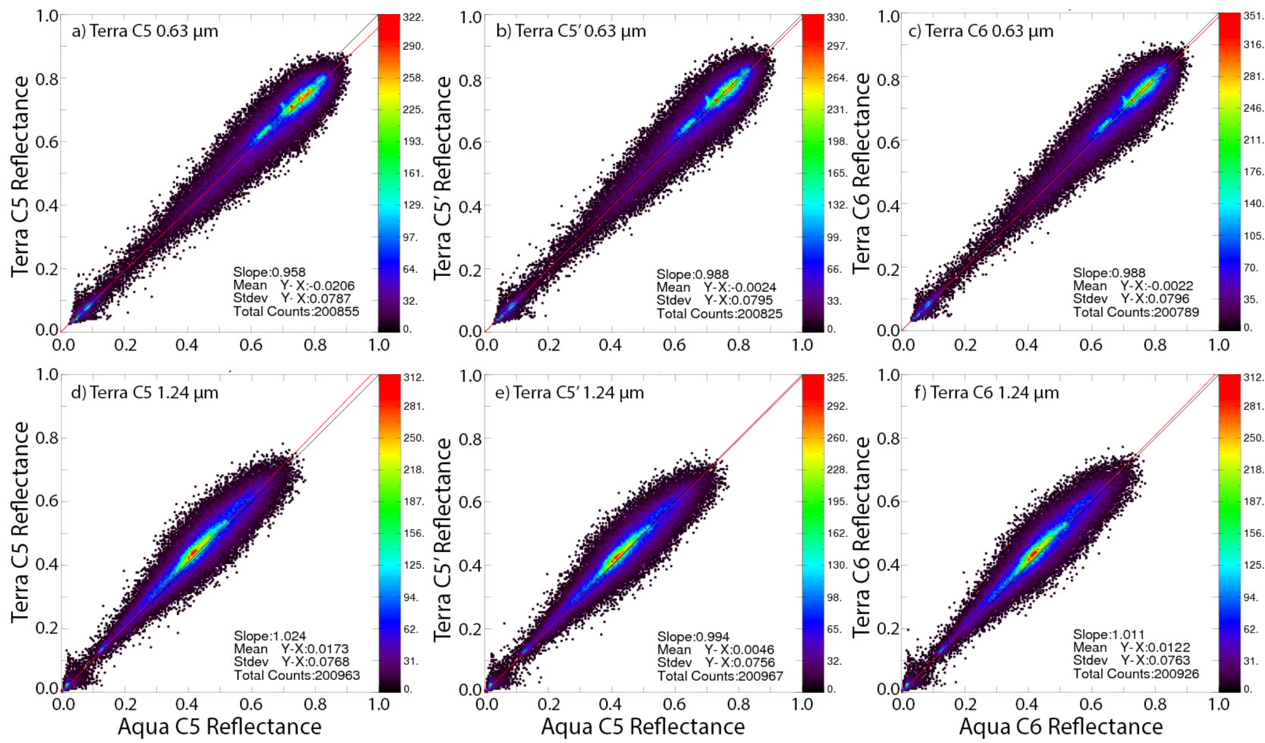

Fig. 2. Reflectance comparisons between the matched Terra and Aqua data during April 11, 2015. All Aqua data on the x-axis are at the same wavelengths as the Terra data. Colors: number of 50-km pixels averages for each reflectance pair. Data on the y-axis are Terra (a) C5 0.63-μm, (b) adjusted C5, C5', 0.63-μm, (c) C6 0.63-μm, (d) C5 1.24-μm, (e) C5' 1.24-μm, and (f) C6 C5 1.24-μm data. Slope is for force fit (red) line through origin. PX and PY are the mean Aqua and Terra reflectances, respectively. Stdev is the standard deviation of the differences. The number of samples varies because of differences in meeting the reflectance limits of 0.0 and 1.0.

(VIS), the Terra reflectances are raised by 1.0% at the beginning of the Aqua period up to 3.2% after March 31, 2009. These adjustments roughly coincide with the Terra MODIS solar diffuser door being permanently open beginning in July 2, 2003, and a Terra MODIS solar diffuser correction applied in early 2009 that resulted in a total degradation of 1.5% [20].

Fig. 2 compares reflectances from Terra C5, Terra C5', and Terra C6 at 0.63 (top) and 1.24 μm (bottom) with the matched Aqua C5 data for April 11, 2015. In Fig. 2, the scatter density plots are shown with the line of agreement (black) and the linear fit to the data (red), as well as the statistics of the linear fits forced through the origin. Given the assumption that zero reflectance at 0.000 is true for all of the calibrations, the linear fits were performed by forcing the intercept to be (0.000, 0.000) for all sets of matched data. This eliminates the impact of a varying intercept on the computed slope, facilitating the analysis of trends in the fits. The slopes range from 0.958 for the C5 pairs [Fig. 2(a)] to 0.988 for both the C5'–C5 [Fig. 2(b)] and C6–C5 [Fig. 2(c)] matches for channel 1 (0.63 μm) and from 0.994 for C5'–C5 [Fig. 2(e)] to 1.024 for C5–C5 [Fig. 2(d)] for channel 5 (1.24 μm). The C6–C5 1.24-μm slope [Fig. 2(f)] is midway between the other two. The magnitude of the mean 0.63-μm reflectance differences between Terra C5 and Aqua C5 is an order of magnitude greater than those from the other two combinations. At 1.24 μm, the C5–C5 and C6–C5 differences are 0.017 and 0.012, respectively, and are noticeably greater than the 0.005 C5'–C5 difference. The standard deviations of the differences are essentially the same for all cases.

Fig. 3 shows the time series of the slope and mean difference results for the channel 1 data based on the selected daily matches. The C5–C5, C5'–C5, and C6–C6 values are indicated in blue, red, and green, respectively. Slopes and reflectance differences for each day are presented in Fig. 3(a) and (c), respectively. Both quantities show a fairly systematic annual cycle that tends to a maximum around the beginning of each year and bottoming out late during each year. This seasonal "cycle" most likely reflects the varying angular configurations of the matched data sets, as well as the changing surface types viewed in the matching zones. The matches occur only over polar regions. During the beginning of the year, most of the matches are in the Southern Hemisphere near or over Antarctica, while the middle of the year is dominated by scenes over the Arctic. In addition to the annual cycle of viewed geography, it is probable that the angular differences in the selected data are seasonally dependent because of the liberal angular and time allowances used here to match the data. That is, the average differences in time and, therefore, SZA, viewing zenith angle, or relative azimuth angle between the two satellites may systematically vary with season, with the sign of a given difference flipping at some point as the intersatellite configuration changes over the year. Systematic angular differences between Terra and Aqua will cause biases

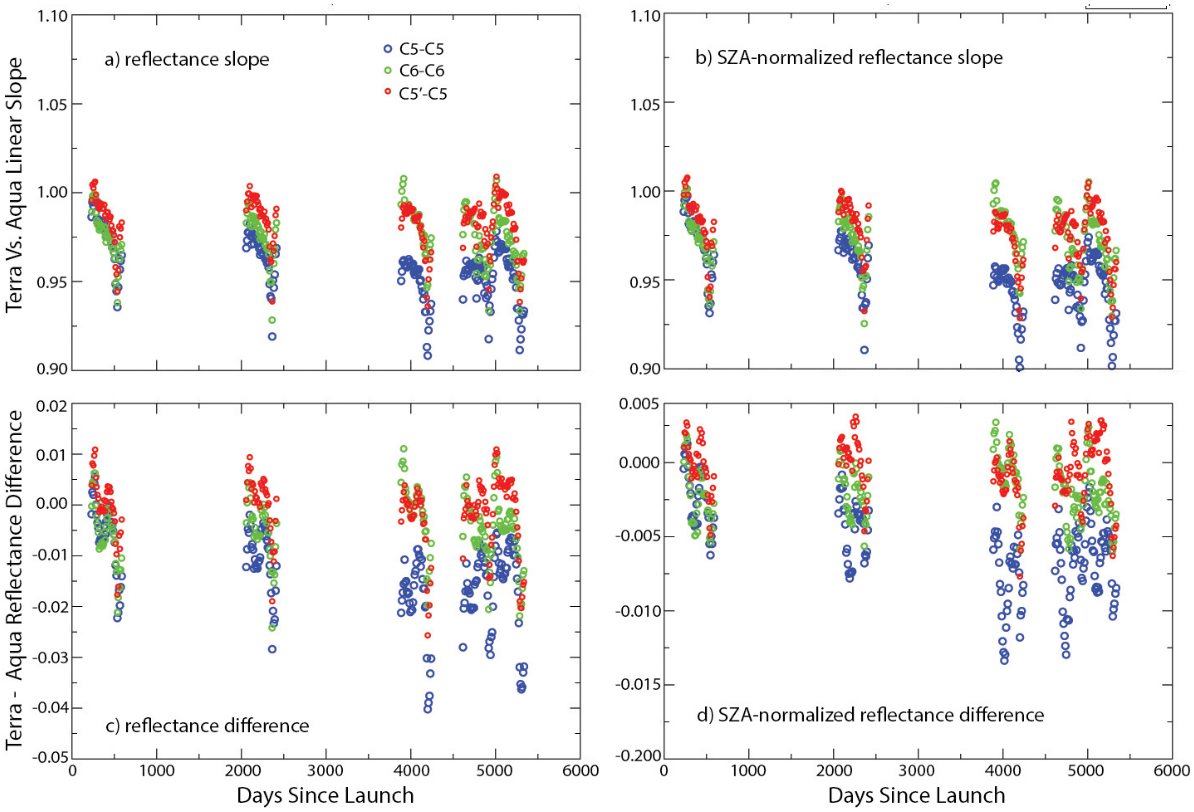

Fig. 3. (Top) Daily forced-fit linear slopes and (Bottom) reflectance differences for various versions of Terra MODIS collections (C5, C5', and C6) versus Aqua MODIS C5 and C6 reflectances for channel 1 (0.63 μm) from matched data sets taken days 1, 11, and 21 of each month during 2003, 2008, 2013, 2015, and 2016. Differences are T–A. SZA-normalized reflectances are measured reflectances multiplied by the cosine of the SZA. Days since launch are measured relative to the launch of Aqua, May 14, 2002.

between the two reflectance sets, because the bidirectional reflectance from a given scene is highly anisotropic (see [24]). Those biases will vary as the average angular configuration differences change over the seasons. Using the annual average should account for those seasonal changes and should be unbiased on the whole. Doelling *et al.* [22] applied much tighter restrictions for matching Terra and Aqua to compute slopes for each month between 2002 and 2012. Their results show no seasonal cycles similar to those observed here, indicating that the angular configurations are the likely culprit for the apparent seasonal changes in gain.

The data sets in Fig. 3(a) are closest during the initial period, although the C5' results tend to have the greatest values. The slopes are separated by 2008 (days 2050–2466), although the C5' and C6 differences are relatively close. Slope and difference separations are the greatest around day 4000 when the C5 values are markedly less than their C5' and C6 counterparts. The C5' and C6 results remain fairly close during the past 2 years.

To put the results on a roughly equivalent radiance basis (Earth–Sun distance variations are neglected), the reflectances were multiplied by cos(SZA). The slope behavior [Fig. 3(b)] is a bit cleaner than the unnormalized results, but remains essentially the same as the unnormalized data. The magnitude of the differences in the normalized reflectances decreases significantly and the separation of the C5 values from the others is a little clearer. Despite the variability during the year, it is evident that the Terra C5' and C6 reflectances are relatively close, particularly during the latter years, and exceed their C5 reflectances, which are consistently less than their Aqua counterparts.

This behavior is seen more clearly in the annual means. These are shown in Fig. 4 for channels 1, 5, 7, and 26 using the SZA-normalized reflectances. The C5 and C6 0.63-μm slopes [Fig. 4(a)] and differences [Fig. 4(b)] are nearly equal during 2003 and diverge afterward, with the C6 means remaining fairly constant between 0.97 and 0.98 over 15 years. The mean differences [Fig. 4(b)] mimic the slopes. The C5' differences are near zero during 2003, 2008, and 2016, but drop to almost -0.002, below the C6 mean, in 2013. The C5 minimum difference of almost -0.008 also occurs during 2013. The C6 differences average out to approximately -0.002 with a maximum in 2013. Overall, the interannual variability is reduced significantly in the C5'–C6 and C6–C6 differences relative to their C5–C5 counterparts. Remaining variability in the former differences is probably due mainly to unresolved calibration differences and, possibly, incomplete angular configuration sampling in some years. It is assumed that the corrections from 2009 hold afterward. However, both the Terra and Aqua calibrations changed after 2009, particularly after 2012 [22].

The interannual varibility in channel 5 is less dramatic than for channel 1. The slopes [Fig. 4(c)] for C5 and C6 are very similar, ~1.005, except during the past 2 years when the

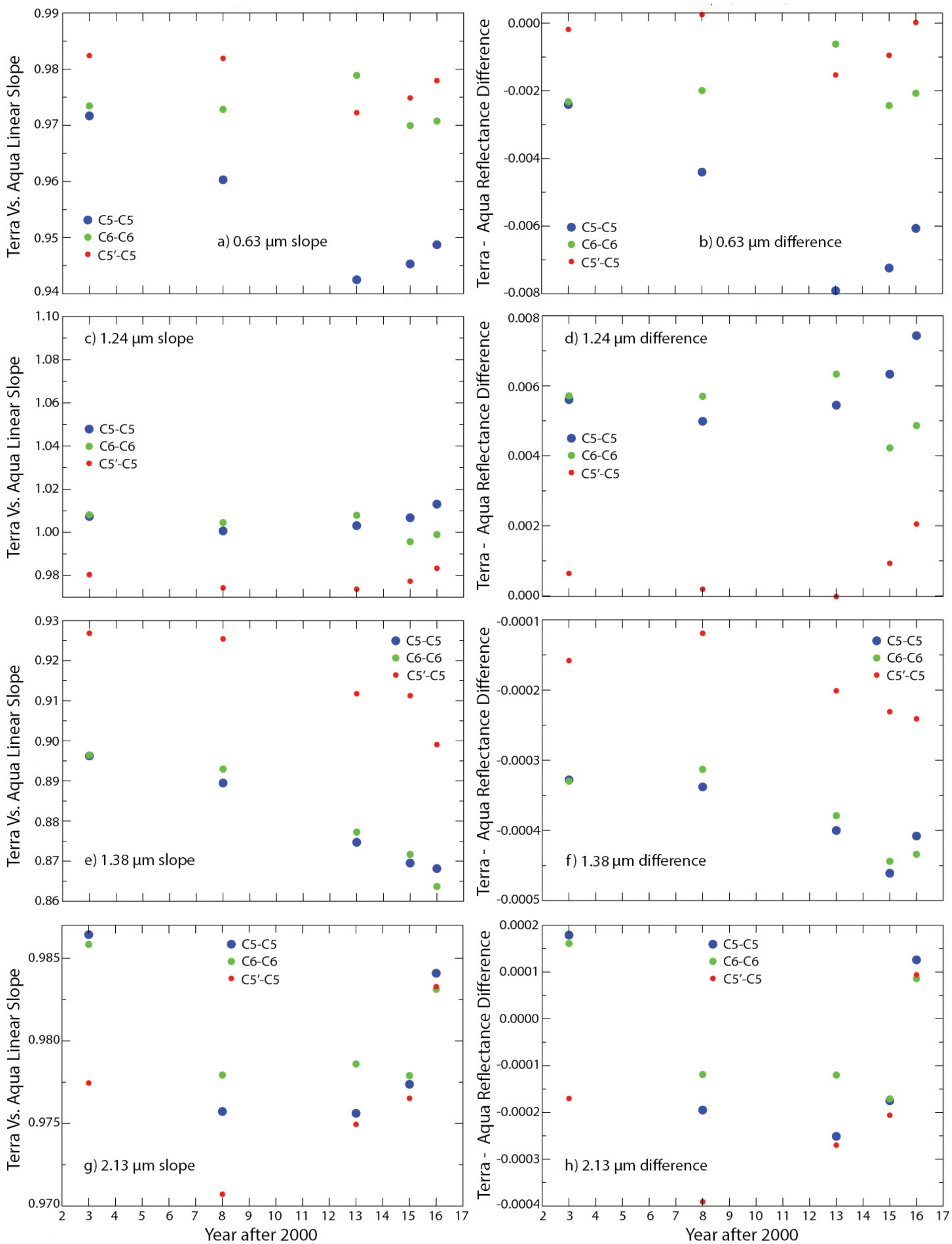

Fig. 4. (Left) Annual mean forced-fit linear slopes and(Right) reflectance differences for various versions of Terra MODIS collections (C5, C5', and C6) versus Aqua MODIS C5 and C6 reflectances (see Fig. 3) for channels (a) and (b) 1, (c) and (d) 5, (e) and (f) 26, and (g) and (h) 7 from 36 days of matched data sets taken each year. Differences are T–A. All quantities are SZA normalized.

C6 values dip below the C5 slopes. The C5' slope is fairly steady around 0.98. The original Terra C5 calibration produces mean normalized reflectance differences of ~0.006 relative to Aqua C5 [Fig. 4(d)], a value similar to the C6 differences before 2014. A change in the T–A relationship must have occurred between 2013 and 2015, as the C6 differences dropped to 0.004, while the C5' values rose from near zero to 0.002.

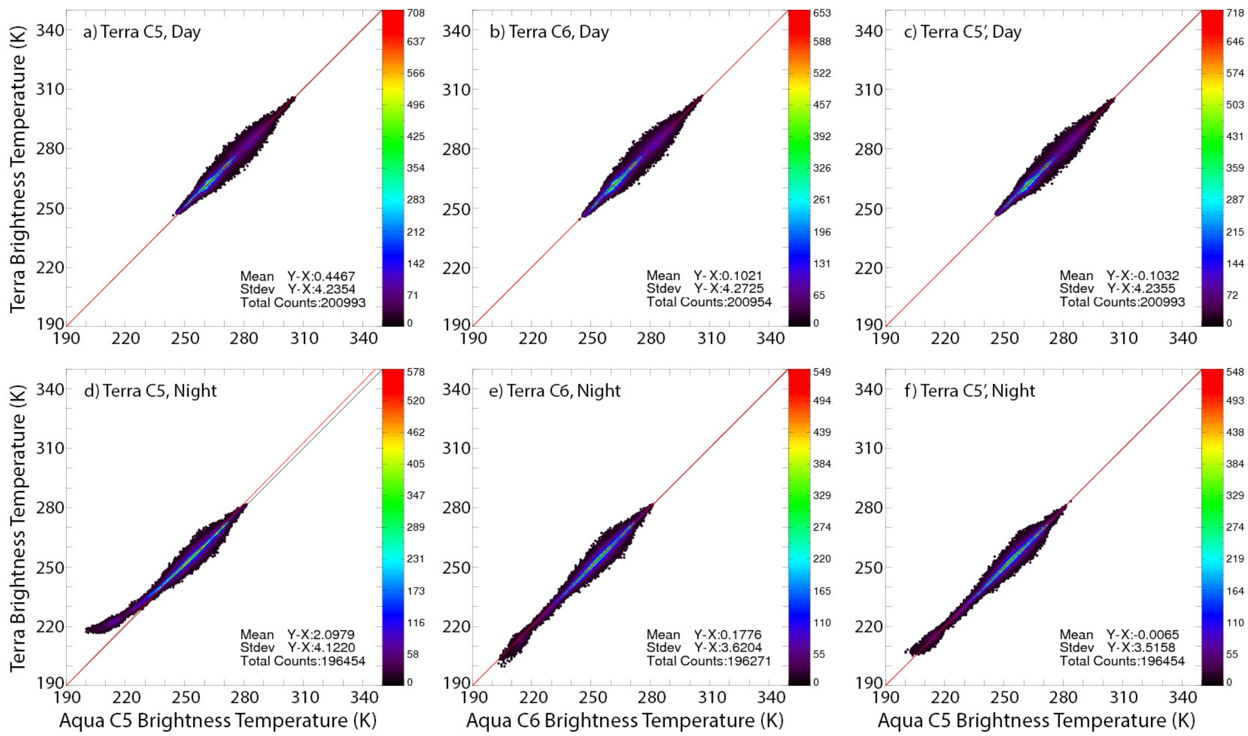

Fig. 5. Same as Fig. 2, except for shortwave infrared (3.8 μm) brightness temperatures and their differences. (Top) Daytime. (Bottom) Night.

Channel 26 is somewhat like channel 5 in which it appears that few changes were made to the Terra calibration between C5 and C6, as their slopes [Fig. 4(e)], and differences [Fig. 4(f)] relative to the matched Aqua data are very close throughout the study period. The differences drop from -0.0003 to almost -0.0005, while the slopes decrease by $\sim$0.04. The C5' slopes and differences drop by almost 0.03 and from -0.00012 to -0.00025 during the same time. While these values seem quite small, the mean reflectance for channel 26 is $\sim$ 0.01, so a 0.0002 difference is a 2% bias. Because channel 26 is so sensitive to water vapor absorption by very narrow lines, small differences in the SRFs could produce significant differences in reflectance. The impact of the SRFs on the T–A relationships was estimated from calculations performed using the spectral integration computational system of [25] for spectral data over the polar regions. It was found that, except for channel 26, the SRF differences produce ratios of 0.999–1.003. For the 1.38-μm channel, however, the SRF differences yield a correction of 1.014, a value roughly one-third that in Table II. Thus, the correction used for Ed4 may over adjust the Terra reflectances by a third too much. Nevertheless, the correction should improve the A–T channel-26 consistency relative to that from the C5 and C6 data.

At 2.13 μm, the C5 and C6 slopes [Fig. 4(g)] and differences [Fig. 4(h)] are again very similar, but not as close as for 1.38 μm. In this case, the adjustments to C5, seen in the C5' results, appear to have diminished the consistency of the Terra and Aqua channels between 2008 and 2015, and possibly, for some years prior to 2008 as the slopes are the smallest and the magnitudes of differences greatest for those periods. Relative to the mean reflectance, the C5' differences convert to approximately -1%. For this band, the Terra C6 calibration appears to be most consistent with Aqua with a mean difference near zero.

For the evaluations in Figs. 3 and 4, is the annual average difference a reliable reference? Here again, the results of [22] provide reference points for comparison of the results. Doelling *et al.* [22, Table IV] listed the normalization slopes and their trends and means for the period 2002–2012. Their average values for both the nadir matches and off-nadir matches are reproduced in Table III along with the averages computed for the same time period using the coefficients in Table II. The mean Ed4 values for channels 1, 4, 5, 7, and 27 are all within $\pm$0.2% of the presumably more accurate, previously published values. For channels 2 and 3, the Ed4 coefficients underestimate gain change by 0.6% and 1.0%, respectively. Fortunately, for the Ed4 cloud retrievals, those two channels have only a small influence on the results. In general, therefore, there should be minimal differences between the Terra and Aqua products due to intercalibration discrepancies in the solar channels, at least, through 2012. This is what the mean differences in Fig. 4 show. While the C5'–C5 annual mean differences are all quite close to zero, the mean slopes, are not as close to the predicted values (Table II) as would be expected. Slopes, being ratios for forced fits, are not linearly related and would not be expected to produce the correct result through linear averaging. Thus, the mean difference is a more reliable metric for the evaluation.

TABLE III
MEAN CALIBRATION COEFFICIENTS FOR TERRA MODIS C5, JUNE 2002–DECEMBER 2012

Channel	Doelling et al. [22] nadir (off)	CERES Ed4 Clouds
1 (0.65 μm)	1.021 (1.021)	1.022
2 (0.87 μm)	1.008 (1.007)	1.002
3 (0.47 μm)	1.023 (1.018)	1.011
4 (0.55 μm)	1.012 (1.012)	1.013
5 (1.24 μm)	0.970 (0.971)	0.972
7 (2.13 μm)	0.999 (0.999)	0.997
26 (1.38 μm)	1.041 (1.039)	1.041

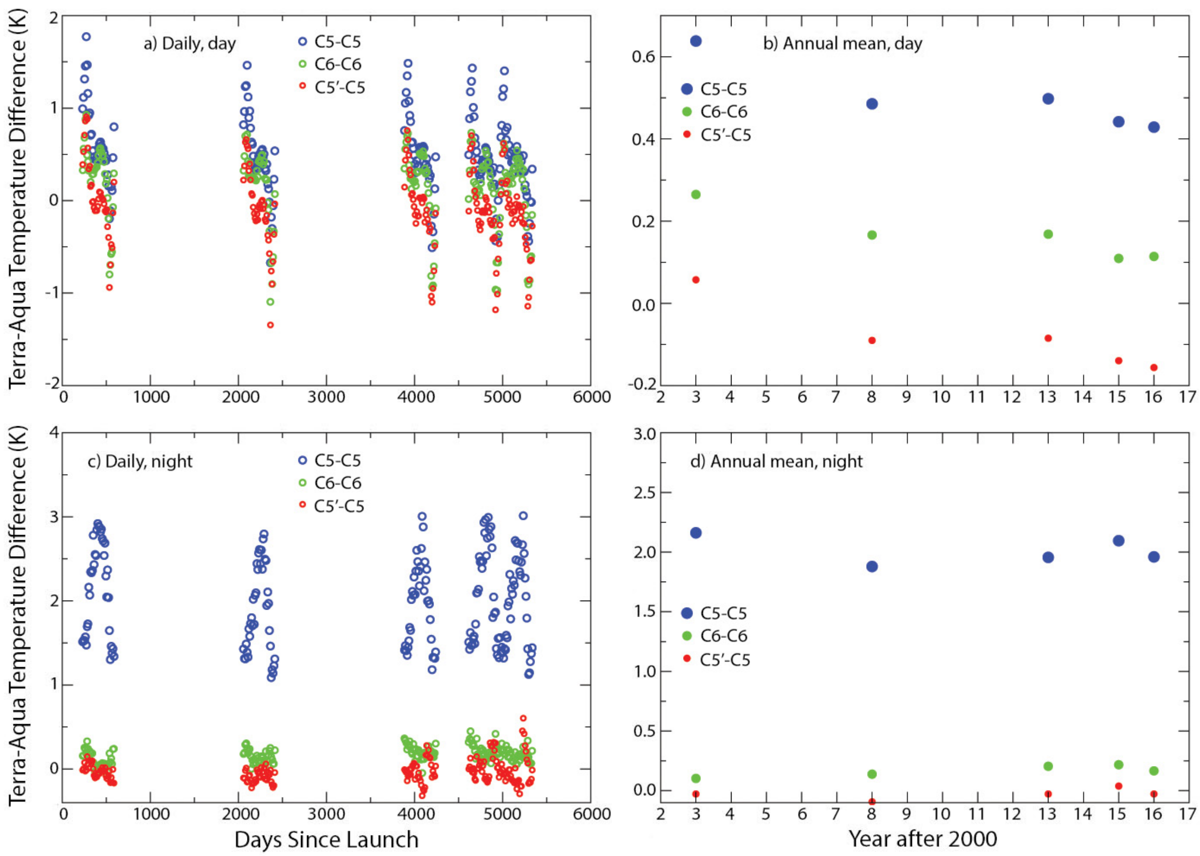

Fig. 6. (Left) Daily and (Right) annual mean and differences between various versions of Terra MODIS collections (C5, C5', and C6) minus Aqua MODIS C5 and C6 brightness temperatures (see Fig. 3) for channel 20 (3.8 μm) from 36 days (top) and nights (bottom) of matched data sets taken each year. All differences are T–A.

B. Shortwave Infrared Channel

The changes in the Terra C5 SIR channel calibration also result in much greater consistency between Terra and Aqua. Fig. 5 shows comparisons of matched Terra and Aqua Channel-20 brightness temperature data for day (top) and night (bottom), April 11, 2015. During the day, the original C5 temperatures [Fig. 5(a)] differ by ~0.5 K, a value close to that reported in [13]. The C6 data [Fig. 5(b)] yield a smaller difference, $T_{\mathrm{Te}} - T_{\mathrm{Aq}}$, of 0.1 K suggesting that the Terra calibration changed for C6 over the observed range. The CERES adjustment applied to the C5 data during the daytime [Fig. 5(c)] also reduces $|T_{\mathrm{Te}} - T_{\mathrm{Aq}}|$ to less than 0.1 K. At night, the Terra C5 temperatures [Fig. 5(d)] asymptote at ~220 K, while T_{Aq} drops to values as low as 200 K, as seen earlier. The mean difference is 2.1 K. The C6 calibrations [Fig. 5(e)] straighten the curve, resulting in much better agreement, a difference of 0.2 K, between Aqua and Terra at the low temperatures. Applying the CERES corrections to T_{Te} [Fig. 5(f)] also results in excellent agreement with a 0.0-K mean differences. The C6 and C5' standard deviations are less than their C5 counterpart.

These results are fairly typical. Fig. 6 plots the daily and monthly mean temperature differences between Terra collections C5, C5', and C6 and their Aqua C6 counterparts. The daytime daily differences [Fig. 6(a)] for all Terra versions have distinct seasonal variations, ranging over ~2 K. The peak occurs around February and the minimum around November. The C5'–C5 nocturnal differences [Fig. 6(c)] have a distinct

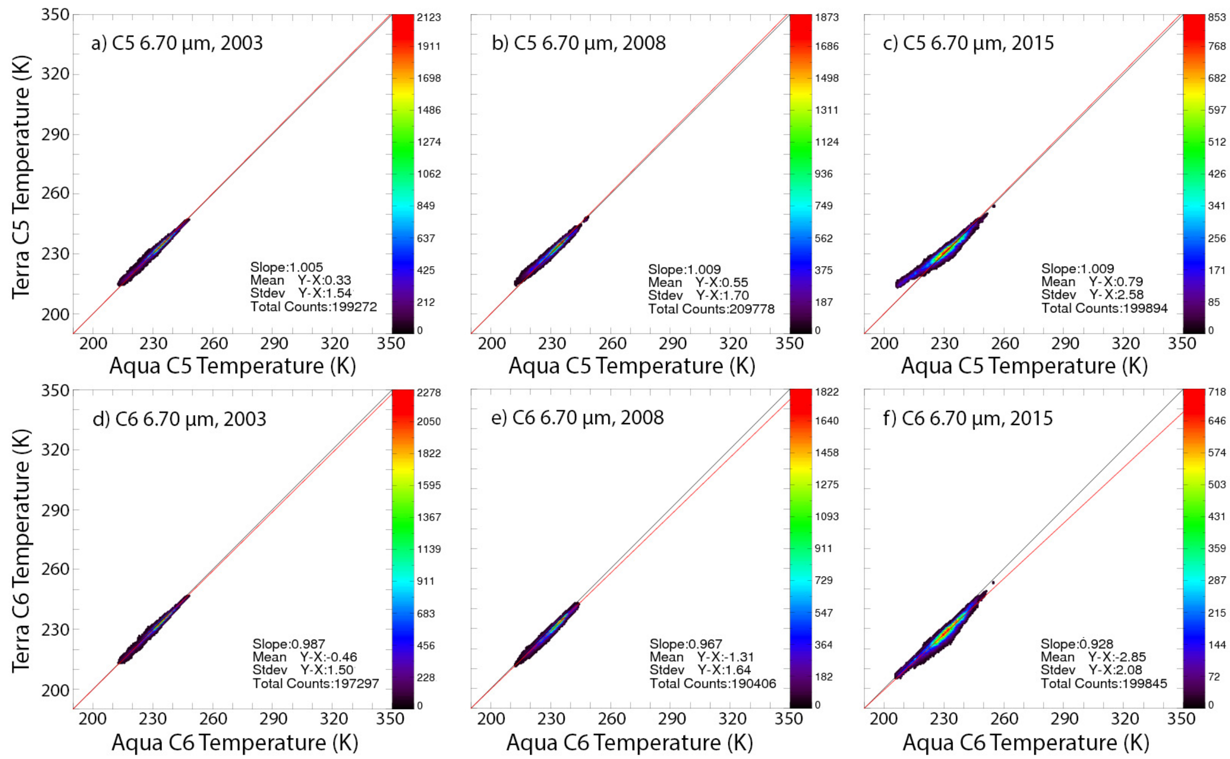

Fig. 7. Channel 27 brightness temperature comparisons between matched Terra and Aqua data at night during 11 July for three different years. (Top) C5 data. (Bottom) C6 data.

variation of ∼1.5 K each year with minima in January and December with a peak near the boreal summer soltice. For the C6–C6 and C5'–C5 values, the seasonal cycles are reduced to ∼0.3 K and have a slightly different phasing. Since the 3.8-μm channel has a solar reflected component, it follows the same seasonal pattern as the visible channel during the daytime (Fig. 3). The nighttime seasonal variation in the C5–C5 differences is due to disparity in the relative frequency of very low temperatures observed over the Arctic and Antarctic, the latter being colder, on average.

The trends are clearer in the annual means. The average daytime [Fig. 6(b)] C5 T–A difference decreases from 0.65 K in 2003 to 0.45 K in 2016, while the C6–C6 and C5'–C5 differences drop from 0.27 to 0.12 K and from 0.06 to −0.16 K, respectively. At night [Fig. 6(d)], the C5–C5 differences hover around 2.0 K. The C6 and C5' Terra mean temperatures differ from their Aqua counterparts by roughly 0.2 and 0.0 K, respectively. No trend is evident in the nighttime differences.

C. Longwave Infrared Channels

Although no changes were applied to the longer wavelength channels, it is instructive to examine the intersatellite consistency of the relevant channels to understand their potential impact on any retrievals. The monthly comparisons between Terra and Aqua MODIS channels were performed for the period 2002–2016. The results are summarized here using daytime and nighttime data together.

1) Channels 27 and 29: The primary water vapor band, channel 27, showed some changes over time as reported in [26] and shown in Figs. 7 and 8 for nighttime and daytime data, respectively. At night, the Aqua and Terra 6.78-μm temperatures were very close on July 11, 2003 in both the C5 [Fig. 7(a)] and C6 [Fig. 7(d)] data, but by 11 July 2008, the Terra C5 temperatures [Fig. 7(b)] were slightly less than their Aqua counterparts at the low end resulting in a mean temperature differences of 0.55 K. By July 11, 2015 [Fig. 7(c)], the difference at the low end increased, resulting in a bias of 0.8 K. The C6 adjustments appear to have corrected the low-end bias but decreased the upper end resulting in average T–A differences of −1.3 and −2.9 K by July 11, 2008 and 2015, respectively. The forced linear fits dropped from 0.987 in 2003 to 0.928 in 2015. During daytime, when the matched data were taken mostly in the northern polar regions, the lowest end of the range is not represented and the differences are no longer positive, on average. On July 11, 2003, the daytime C5 and C6 mean biases are −0.2 and −0.7 K (not shown), respectively. By 2015, the differences are strongly negative for both C5 [Fig. 8(a)] and C6 [Fig. 8(b)]. Combining the day and night data tends to favor the upper end of the scale.

The trends in the channel-27 T–A differences are more evident in the time series of monthly mean differences plotted in Fig. 9 for the combined day and night matched data. The average C5 difference [Fig. 9(a)], which reflects the degree of low-end divergence, begins slightly positive and gradually falls below zero to around −1 K by 2015. During 2016, the differences drop suddenly in mid-February and do not recover, as first reported in [26]. The C6 trend [Fig. 9(b)] is much steeper, beginning with a small negative value and

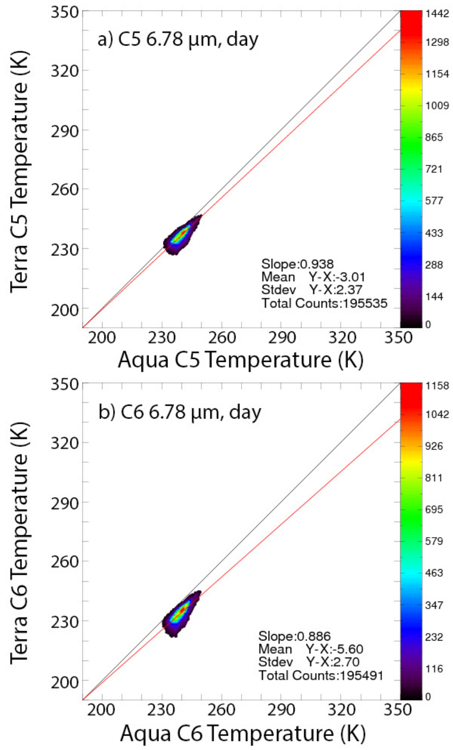

Fig. 8. Channel 27 brightness temperature comparisons between matched Terra and Aqua data in daytime during 11 July 2015. (a) C5 data, (b) C6 data.

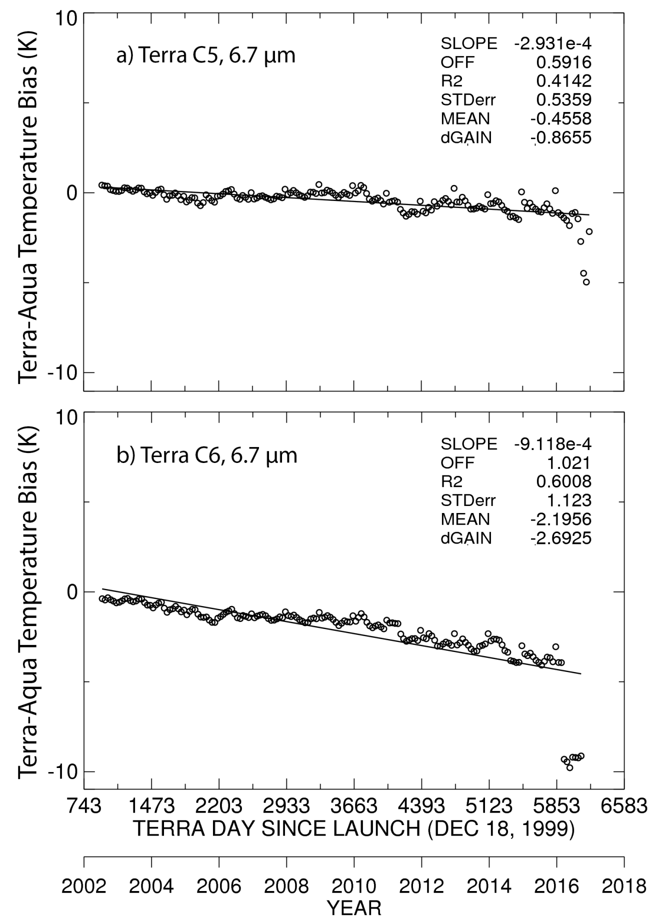

Fig. 9. Channel 27 monthly mean brightness temperature differences between matched Terra and Aqua data. (a) C5 data. (b) C6 data.

reaching nearly 4 K in mid-2015. Apparently, the C6 revision of the 6.78-μm channel corrected the low-end bias (Fig. 7) with the effect of causing a bias at higher temperatures. The drop during February 2016 is much more evident in the C6 data and suggests that the Terra channel-27 data taken after the plunge should not be used as they are poorly correlated and have significant interdetector striping (not shown).

Fig. 10 presents scatter plots and fits for the same T–A matches seen in Fig. 7, except that the channel-29 (8.55 μm) data are used. The C5 data are well correlated linearly in 2003 [Fig. 10(a)] with mean difference of 0.4 K. The linear structure gives way over time to positive biases in Terra at the low end of the range resulting in average differences of 0.9 K in 2008 [Fig. 10(b)] and 3.2 K in 2015 [Fig. 10(c)] for these 11 July matches. Calibration adjustments used for the C6 collection appear to have eliminated most or all of the differences through 2015 as the linear structure is retained in Fig. 10(d)–(f) and the magnitude of the mean differences is 0.2 K or less in these examples. The monthly mean T–A differences in Fig. 11 are near zero before 2008 and then rise to values greater than 3 K by late 2015 [Fig. 11(a)]. The linear fit of the trend produces a slope that is $3\times$ that of the fit to the C6 data [Fig. 11(b)]. For the latter, the mean difference starts as a small negative value that becomes positive over time and bumps up by $\sim$0.5 K in 2016 to 1 K.

2) Channels 31, 32, 33: For C5, the mean difference between Terra and Aqua for the entire period at 10.8 μm (channel 31) is 0.05 K. For the 12.0- and 13.4-μm channels, the average differences are 0.02 and -0.05 K, respectively. No significant trend in the differences was found for any of the three channels. The C6 consistency is similar. For channels 31, 32 (12.0 μm), and 33 (13.4 μm), the T–A differences are -0.07, -0.09, and -0.12 K, respectively. Again, no trends in the differences were observed. The fitted linear slopes typically differed from 1.000 by less than $\pm 1\%$ for both collections, indicating that the consistency between Terra and Aqua occurred at all values.

IV. Calibration Impact on Retrieved Cloud Properties

The above-mentioned comparisons indicate that when corrections were applied to the C5 data for CERES Ed4, they generally resulted in a T–A radiance consistency that is as good as or better than that of the C6 data sets. When corrections were neither developed nor applied, some artifacts are likely to be introduced into the Ed4 cloud property record. For example, the solar channel corrections were developed using the Aqua data and were only applied during the Aqua period. The pre-Aqua period for Terra could produce an anomaly because of the absent corrections. These and other aspects of the Terra and Aqua calibrations are discussed as follows. While it is beyond the scope of this paper to illustrate the impact of the calibration changes on all of the various cloud properties, a few examples are given to highlight the importance of the corrections.

The examples presented below are based on averages of the selected cloud properties computed from all MODIS pixels

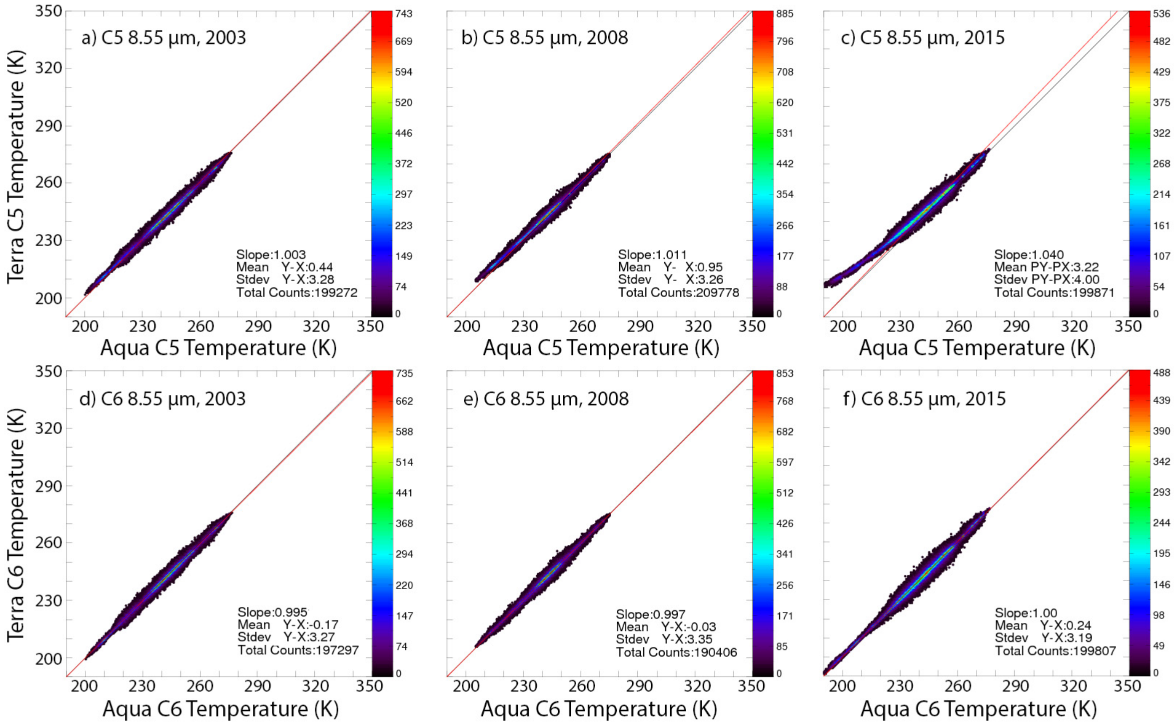

Fig. 10. Same as Fig. 7, except for Channel 29.

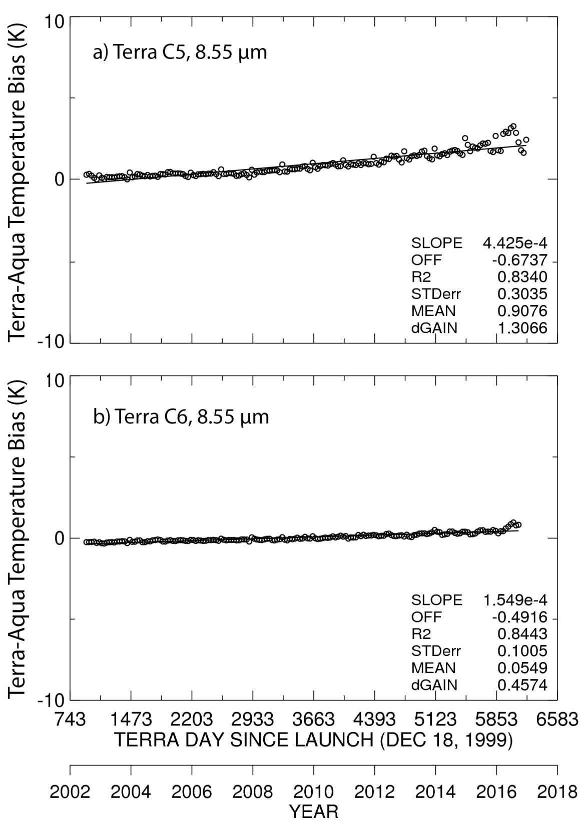

Fig. 11. Same as Fig. 9, except for MODIS channel 29. (a) Terra C5, 8.55 μm. (b) Terra C6, 8.55 μm.

satisfying the particular criteria for each satellite and CERES edition within a given month. Twelve-month running means were then computed from the monthly means and plotted for the particular category. The plots also include the standard error of the 12-month means to indicate the seasonal variability. Save for the one polar exception noted in the following, both the Terra and Aqua Ed2 algorithms are the same. The Ed4 algorithms differ from those of Ed2, but they are identical for the two satellites. Ed2 uses the C5 data for both satellites, while Ed4 uses C5 for Aqua and C5' for Terra. Thus, the intersatellite differences for a given edition are due, in part, to the local time difference of the satellite overpasses and cannot be expected to be exactly the same. The differences can also be due to intersatellite calibration discrepancies. Long-term trends in the Aqua and Terra parameters should be similar if the satellites are consistently calibrated since the trends can be assumed to be governed by large-scale changes.

A. Solar Channels

Because channel 1 is the primary solar channel used for cloud detection and optical depth retrieval over nonsnow surfaces in both the Ed2 and Ed4 algorithms [13], [17], [19], [27] the calibration of this channel has significant influence on the cloud retrievals. Likewise, over snow, the 1.24-μm channel is the primary channel for optical depth retrieval. Fig. 12 plots the time series of Terra and Aqua CODs for Ed2 based on the C5 data and Ed4 based on the C5' data for both the nonpolar (60° S–60° N latitudes) and polar (poleward of 60° latitude) regions. The mean nonpolar [Fig. 12(a)] Terra Ed2 CODs (shown in gold) are relatively flat in the initial years and have a downward trend after 2003 [Fig. 12(a)], dropping by more than 10% between 2003 and 2012. The trend is not continuous, but tends to reflect the discontinuities assumed in Table II. The Aqua Ed2 CODs (shown in aqua blue) are between 4%

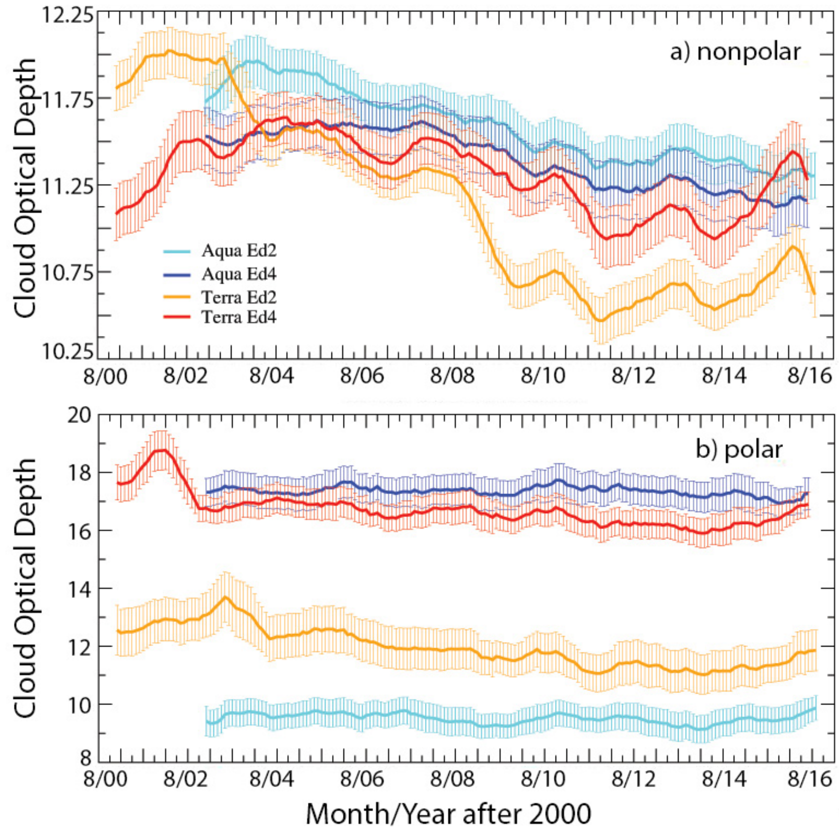

Fig. 12. Twelve-month running mean daytime CODs from CERES-MODIS retrieval algorithms. Bars: standard error of the mean computed for each 12-month period. (a) Nonpolar. (b) Polar.

and 9% greater than their Terra counterparts and have a slower downward trend of −4.1%/dec. Using the C5' calibration for Terra brings the Ed4 COD means for the two instruments into much better agreement. Although there is no particular reason for Terra (shown in red) and Aqua (shown in blue) to have the same average optical depths, they are taken 3 h apart, they would likely have similar trends if their calibrations are consistent. During the pre-Aqua period, the Ed4 Terra COD is up to 4% less than its value at the beginning of the Aqua period. The pre-Aqua differences between the Terra Ed2 and Ed4 CODs are primarily due to the changes in cloud fraction between Ed2 and Ed4. More optically thin clouds were detected in Ed4 than in Ed2, reducing the average optical depth. This effect is also seen the Aqua COD averages, especially in the early years. From the sharp rise in Terra Ed4 COD before the Aqua period, it is clear that the C5' 1% channel-1 calibration adjustment (Table II) should have been extended back to the time of the Terra launch.

Despite the intersatellite consistency in the Ed4 results, the Aqua CODs still have a trend of −3.3%/dec. The Terra Ed4 trend is similar to that for Aqua, if only data after 2002 are considered. This decrease in COD over time is most likely due to degradation in the Aqua channel-1 calibration seen after 2007. Doelling *et al.* [22] showed that the Aqua C6 gain dropped by 1%/dec. Because there were only minor changes between Aqua C5 and C6, the Aqua C5 gain had the same trend. This degradation was not discovered prior to Ed4 processing and was not included in the C5' calibrations. Since the Terra C5' calibration depends on Aqua, the Terra Ed4 CODs decrease at the same rate as the Aqua means as long as other changes do not occur in the Terra calibrations after 2009.

Over the polar regions [Fig. 12(b)], the Ed2 CODs differ by ∼20%. The Terra Ed2 means have a slightly decreasing trend, while their Aqua counterparts remain relatively constant. For Ed2, the Terra 1.6-μm and Aqua 2.1-μm channels were used to retrieve COD over snow. Thus, the differences in the CODs are not surprising as the 2.1-μm reflectance saturates at a lower COD than the 1.6-μm reflectance. In the Ed4 processing, the 1.24-μm channel was used over snow to retrieve COD for both satellites. The resulting mean Terra and Aqua CODs differ by ∼5% and the Terra averages have a negative trend during the Aqua period that is steeper than the −0.16/dec trend in Aqua COD. This suggests that the calibration correction after 2003 should have been larger. The absence of a correction prior to the Aqua launch is evident in the 10% drop in the Terra Ed4 mean COD from 2001 to 2003. The Terra Ed4 results in Fig. 12 suggest that there may be some changes in Terra after 2014 which were not included in Table II. It is likely, therefore, that the greater C5'–C5 differences in Fig. 12 after 2012 are due to adjustments to Terra.

From the examples in Fig. 12, it is clear that reflectance calibration corrections have significant impacts on the retrievals and can either improve or decrease the consistency and

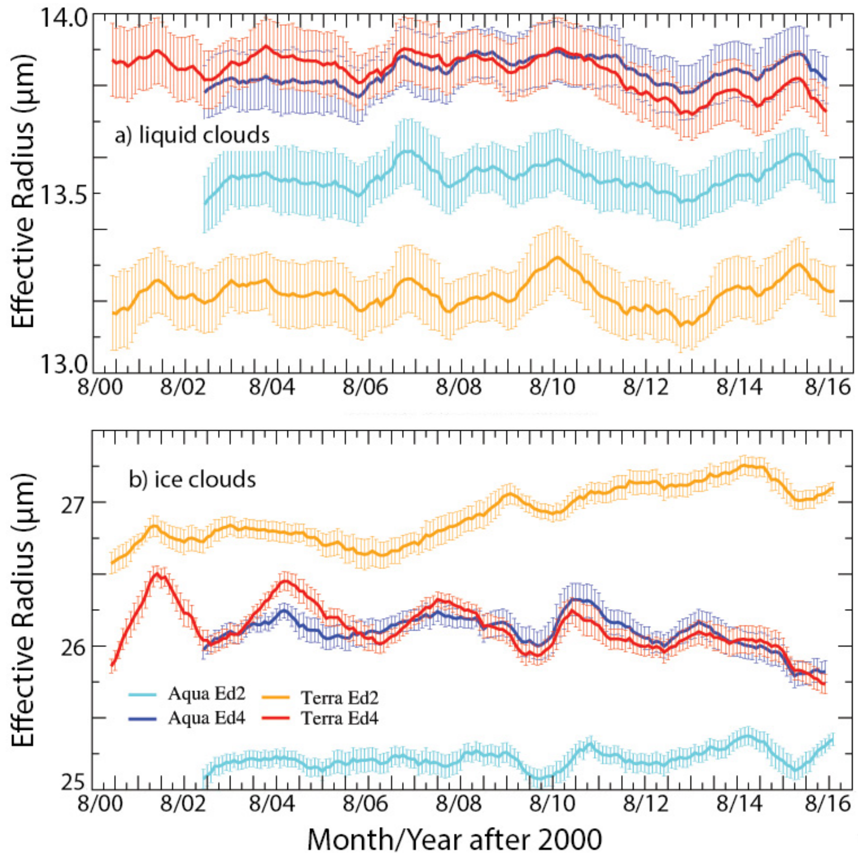

Fig. 13. Same as Fig. 12, except for daytime nonpolar particle effective radius. (a) Liquid clouds. (b) Ice clouds.

accuracy of the results. Impacts due to changes in other solar channels are left for future papers.

B. Shortwave Infrared

Overall, the change in the SIR calibration will tend to affect the Terra cloud particle effective radius, CER, during the day. As seen in Fig. 13(a), the mean Ed2 nonpolar liquid CER from Terra is 0.3–0.4 μm smaller than its Aqua counterpart. For Ed4, the Terra and Aqua CERs differ by less than 0.1 μm. The Terra Ed2 CER for ice clouds is nearly 2 μm greater than the Aqua mean [Fig. 13(b)], but the Ed4 ice CERs are in excellent agreement for nonpolar areas. The increase in the Aqua ice CER from Ed2 to Ed4 is due to the use of a new ice crystal model in the retrieval and some changes in the cloud population. The main point is that the same algorithm is applied to both the satellite data sets and the Ed4 CER values agree much better than the corresponding Ed2 values. Trends of -0.8 and -0.5 %/dec in the Ed4 Terra and Aqua ice CER means are greater than the corresponding -0.5 and -0.2 %/dec for liquid cloud values. Since the CER retrieval depends to some extent on the COD, these trends may simply be the result of the COD trends seen in Fig. 12.

The SIR channel is also used along with many others in the cloud mask and cloud phase selection algorithms. Thus, the impact of the SIR calibration on those other parameters is more complicated than seen for the CER retrieval. These other effects of adjusting the Terra SIR calibration will be discussed in the future reporting.

C. Infrared Channels

The lack of adjustments to the 6.7- and 8.5-μm data also has significant impacts on the CERES Ed4 properties. For example, the 8.5-μm channel is used in the Ed4 phase selection [19], particularly at night. Fig. 14 plots the 12-month running mean, nonpolar fractions of liquid and ice clouds at night. The Terra and Aqua Ed2 mean liquid cloud fractions track each other well and show very little trending. Since the Ed2 phase selection does not employ the 8.5-μm channel, it is unaffected by any of its calibration artifacts. On the other hand, the Ed4 Terra liquid amount appears to decrease slowly between 2000 and 2012, then drops at a much steeper rate through 2016. Meanwhile, the Ed4 Aqua liquid fraction is relatively steady throughout the record with a trend of 0.005/dec. Comparing with the difference trend in Fig. 9(a) (the differences trend for 8.5 μm is similar to that for 6.7 μm (not shown), it is clear that the 8.5-μm channel calibration is the primary cause for the nocturnal phase trend in the Terra Ed4 liquid cloud fraction. This result is not surprising since the 8.5-μm phase selection criteria are based on small brightness temperature differences. Even a tiny calibration trend in one of the two differencing channels calibration is sufficient to bias the results using those brightness temperature differences.

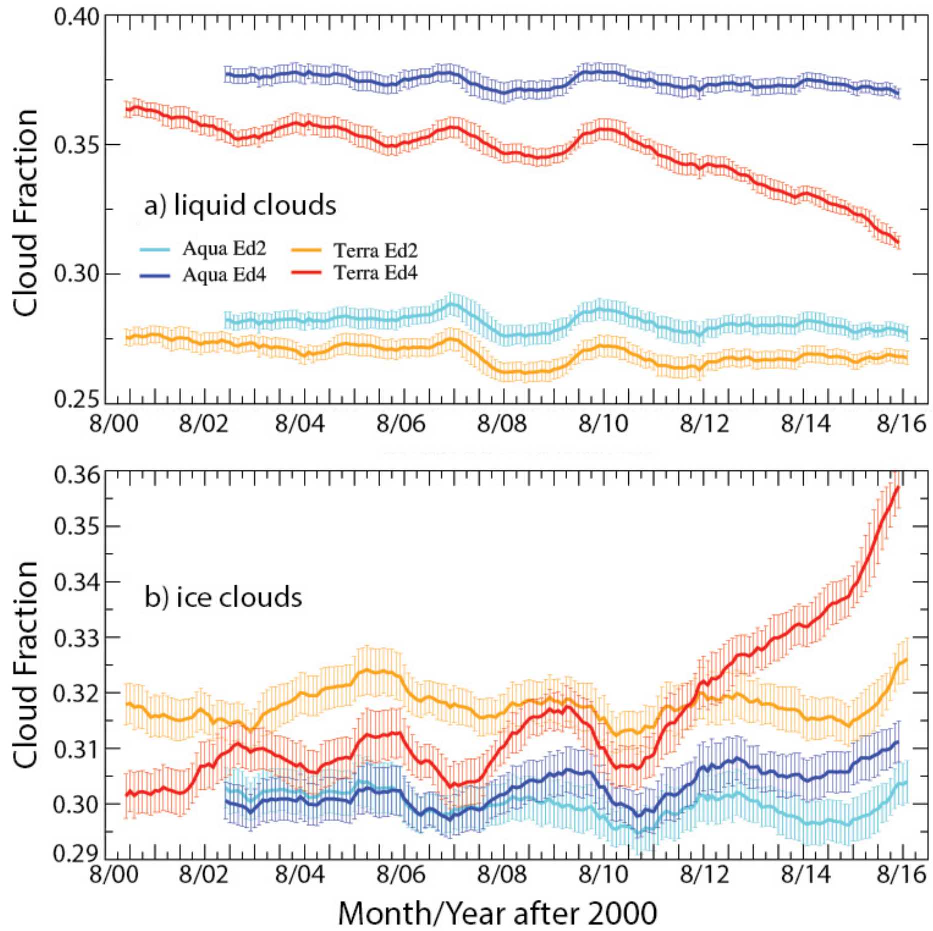

Fig. 14. Same as Fig. 12, except for nighttime cloud fraction over nonpolar regions for each phase.

V. Conclusion

Calibration adjustments were developed and applied to certain Terra C5 channels to account for known differences in Terra C5 and its Aqua MODIS C5 counterparts in order to achieve intersatellite consistency in the CERES Ed4 cloud property retrievals. The main Terra MODIS findings are summarized for each channel as follows.

1) *Channel* 1 *(0.64 μm):* Between July 2002 and 2016, the magnitude of the annual mean T–A reflectance difference after correction is less than 0.002 with an average of less than 0.001. The Terra correction was not applied prior to the Aqua period and does not account for 1%/dec degradation in the Aqua gain after 2008. That degradation remains in the Aqua C6 data [22]. The Terra C6 reflectances, however, appear to be trendless differ from their Aqua counterparts by an average of −0.002 over the record.
2) *Channel* 5 *(1.24 μm):* The T–A reflectance differences for the corrected C5 data after July 2002 are similar to the channel 1 results. No correction was applied to the Terra C5 data before July 2002. A significant T–A bias of 0.006 is present in both the Terra C6 and uncorrected C5 data.
3) *Channel* 7 *(2.13 μm):* The correction applied to the C5 Terra data increased the magnitude of the T–A difference by a factor of 2. The C6 Terra data are more consistent with Aqua C5 than either version of the C5 data.
4) *Channel 20 (3.78 μm):* Biases in the T–A brightness temperature differences have been effectively removed in the corrected Terra C5 data for both day and night. Small T–A biases of ∼0.2 K remain in both the day and night Terra C6 data.
5) *Channel 26 (1.38 μm):* The mean T–A reflectance difference for the corrected data is very small, but still equivalent to −1%. For Terra C6, the difference averages to −3%.
6) *Channel 27 (6.71 μm):* No corrections were applied to the Terra C5 data, but T–A differences at the low end of the temperature range slowly developed and became significant after 2011 in the C5 data. The Terra C6 data show a significant downward trend in T–A beginning in 2002. A large drop in both the Terra C5 and C6 Terra temperatures occurred in 2016.
7) *Channel 29 (8.55 μm):* The Terra C5 data were not corrected and suffered from a gradually increasing T–A temperature difference from 2002 onward. This trend is mostly eliminated in the C6 data.
8) *Channels 31, 32, and 33 (11.0, 12.0, and 13.3 μm):* No corrections were applied to these channels for C5 data. The C5 T–A differences, having a magnitude

of 0.1 K or less, are expected to have minimal impact on the consistency between the Terra and Aqua cloud properties.

All corrections assumed that the relationship between each pair of channels is constant throughout the record and that neither the Aqua nor the Terra MODIS channel calibrations changed after 2009. Analyses in this paper determined that for the channels that were altered, the corrections successfully achieved the desired consistency in both the radiances and Ed4 cloud properties, except when the latter stability assumption was violated. In general, the agreement between the Aqua C5 and adjusted Terra C5 radiances is generally equivalent to or better than that found for their C6 counterparts.

Despite the consistency achieved for the Terra and Aqua data sets in Ed4, the CERES Ed4 SSF-based cloud property data sets should be used cautiously for cloud trend studies. The remaining calibration differences noted earlier have produced some significant artifacts in the cloud properties that affect their use for studying long-term trends in the cloud properties and cloud–radiation interactions. To eliminate those artifacts, it is clear that further adjustments are needed in the MODIS C6 calibrations before reprocessing the CERES cloud properties. Wilson *et al.* [26] recently identified and addressed the problems in the C6 data discussed here for channels 27 and 29. Likewise, Angal *et al.* [28] found the cause of the drift in the Aqua calibration for channels 1–4 and found corrections for it. Those corrections and the adjustments of [26] have been incorporated into a new MODIS L1B radiance data set, C6.1, that is being processed as of this writing [29]. Using that new MODIS collection along with the adjustments to Terra channels 5 and 26 discussed here to reprocess the CERES cloud properties should eliminate the artifacts in the cloud property record noted here and elsewhere.

REFERENCES

[1] B. A. Wielicki *et al.*, "Clouds and the Earth's Radiant Energy System (CERES): Algorithm overview," *IEEE Trans. Geosci. Remote Sens.*, vol. 36, no. 4, pp. 1127–1141, Jul. 1998.

[2] C. J. Stubenrauch *et al.*, "Assessment of global cloud datasets from satellites: Project and database initiated by the GEWEX radiation panel," *Bull. Amer. Meteorol. Soc.*, vol. 94, no. 7, pp. 1031–1049, Jul. 2013, doi: 10.1175/BAMS-D-12-00117.

[3] M. J. Foster *et al.*, "State of the climate in 2015," *Bull. Amer. Meteorol. Soc.*, vol. 97, pp. S28–S29, Aug. 2016.

[4] M. J. Foster *et al.*, "State of the climate in 2016," *Bull. Amer. Meteorol. Soc.*, vol. 98, pp. S27–S28, Sep. 2017.

[5] M. H. Zhang *et al.*, "Comparing clouds and their seasonal variations in 10 atmospheric general circulation models with satellite measurements," *J. Geophys. Res., Atmos.*, vol. 110, no. D15, p. D15S02, 2005, doi: 10.1029/2004JD005021.

[6] D. Waliser *et al.*, "Cloud ice: A climate model challenge with signs and expectations of progress," *J. Geophys. Res., Atmos.*, vol. 114, no. D8, p. D00A21, 2009, doi: 10.1029/2008JD010015.

[7] R. E. Stanfield *et al.*, "Assessment of NASA GISS CMIP5 and post-CMIP5 simulated clouds and TOA radiation budgets using satellite observations. Part I: Cloud fraction and properties," *J. Climate*, vol. 27, no. 11, pp. 4189–4208, 2014, doi: 10.1175/JCLI-D-13-00558.1.

[8] X. Xiong, K. F. Chiang, A. Wu, W. L. Barnes, B. Guenther, and V. V. Salomonson, "Multiyear on-orbit calibration and performance of Terra MODIS thermal emissive bands," *IEEE Trans. Geosci. Remote Sens.*, vol. 46, no. 6, pp. 1790–1803, Jun. 2008.

[9] X. Xiong *et al.*, "Multiyear on-orbit calibration and performance of Terra MODIS reflective solar bands," *IEEE Trans. Geosci. Remote Sens.*, vol. 45, no. 4, pp. 879–889, Apr. 2007.

[10] X. Xiong, J. Sun, X. Xie, W. L. Barnes, and V. V. Salomonson, "On-orbit calibration and performance of aqua MODIS reflective solar bands," *IEEE Trans. Geosci. Remote Sens.*, vol. 48, no. 1, pp. 535–546, Jan. 2010, doi: 10.1109/TGRS.2009.2024307.

[11] X. Xiong, B. N. Wenny, A. Wu, W. L. Barnes, and V. V. Salomonson, "Aqua MODIS thermal emissive band on-orbit calibration, characterization, and performance," *IEEE Trans. Geosci. Remote Sens.*, vol. 47, no. 3, pp. 803–814, Mar. 2009.

[12] P. Minnis, D. R. Doelling, L. Nguyen, W. F. Miller, and V. Chakrapani, "Assessment of the visible channel calibrations of the VIRS on TRMM and MODIS on *Aqua* and *Terra*," *J. Atmos. Ocean. Technol.*, vol. 25, no. 3, pp. 385–400, 2008.

[13] P. Minnis *et al.*, "Cloud detection in nonpolar regions for CERES using TRMM VIRS and Terra and Aqua MODIS data," *IEEE Trans. Geosci. Remote Sens.*, vol. 46, no. 11, pp. 3857–3884, Nov. 2008.

[14] B. N. Wenny *et al.*, "MODIS calibration algorithm improvements developed for Collection 6 Level-1B," *Proc. SPIE*, vol. 7807, pp. 78071F-1–78071F-9, Aug. 2010, doi: 10.1117/12.860892.

[15] X. Dong, P. Minnis, B. Xi, S. Sun-Mack, and Y. Chen, "Comparison of CERES-MODIS stratus cloud properties with ground-based measurements at the DOE ARM Southern great plains site," *J. Geophys. Res., Atmos.*, vol. 113, pp. D03204-1–D03204-17, Feb. 2008, doi: 10.1029/2007JD008438.

[16] P. Minnis *et al.*, "CERES Edition-2 cloud property retrievals using TRMM VIRS and Terra and Aqua MODIS data—Part II: Examples of average results and comparisons with other data," *IEEE Trans. Geosci. Remote Sens.*, vol. 49, no. 11, pp. 4401–4430, Nov. 2011, doi: 10.1109/TGRS.2011.2144602.

[17] P. Minnis *et al.*, "CERES Edition-2 cloud property retrievals using TRMM VIRS and Terra and Aqua MODIS data—Part I: Algorithms," *IEEE Trans. Geosci. Remote Sens.*, vol. 49, no. 11, pp. 4374–4400, Nov. 2011, doi: 10.1109/TGRS.2011.2144601.

[18] G. Toller *et al.*, "Terra and Aqua moderate-resolution imaging spectroradiometer collection 6 level 1B algorithm," *J. Appl. Remote Sens.*, vol. 7, no. 1, p. 073557, 2013, doi: 10.1117/1.JRS.7.073557.

[19] P. Minnis *et al.*, "CERES Edition 3 cloud retrievals," in *Proc. AMS 13th Conf. Atmos. Radiat.*, Portland, OR, USA, Jun./Jul. 2010, pp. 1–7. [Online]. Available: https://ams.confex.com/ams/pdfpapers/171366.pdf

[20] A. Wu, X. Xiong, D. R. Doelling, D. Morstead, A. Angal, and R. Bhatt, "Characterization of Terra and Aqua MODIS VIS, NIR, and SWIR spectral bands' calibration stability," *IEEE Trans. Geosci. Remote Sens.*, vol. 51, no. 7, pp. 4330–4338, Jul. 2013, doi: 10.1109/TGRS.2012.226588.

[21] X. Xiong *et al.*, "Global space-based inter-calibration system reflective solar calibration reference: From Aqua MODIS to S-NPP VIIRS," *Proc. SPIE*, vol. 9881, pp. 98811D-1–98811D-12, May 2016.

[22] D. R. Doelling *et al.*, "The radiometric stability and scaling of collection 6 Terra- and Aqua-MODIS VIS, NIR, and SWIR spectral bands," *IEEE Trans. Geosci. Remote Sens.*, vol. 53, no. 8, pp. 4520–4535, Aug. 2015, doi: 10.1109/TGRS.2015.2400928.

[23] Y. Li, A. Wu, and X. Xiong, "Evaluating calibration of MODIS thermal emissive bands using infrared atmospheric sounding interferometer measurements," *Proc. SPIE*, vol. 8724, p. 87240X, Jun. 2013, doi: 10.1117/12.2016621.

[24] P. Minnis and E. F. Harrison, "Diurnal variability of regional cloud and clear-sky radiative parameters derived from GOES data, Part III: November 1978 radiative parameters," *J. Climate Appl. Meteorol.*, vol. 23, pp. 1032–1052, Jul. 1984.

[25] B. R. Scarino *et al.*, "A Web-based tool for calculating spectral band difference adjustment factors derived from SCIAMACHY hyperspectral data," *IEEE Trans. Geosci. Remote Sens.*, vol. 54, no. 5, pp. 2529–2542, May 2016.

[26] T. Wilson *et al.*, "Development and implementation of an electronic crosstalk correction for bands 27–30 in Terra MODIS collection 6," *Remote Sens.*, vol. 9, no. 6, p. 569, 2017, doi: 10.3390/rs9060569.

[27] Q. Z. Trepte, P. Minnis, C. R. Trepte, S. Sun-Mack, and R. Brown, "Improved cloud detections in CERES Edition 3 algorithm and comparison with the CALIPSO Vertical Feature Mask," in *Proc. AMS 13th Conf. Atmos. Rad. Cloud Phys.*, vol. 32. Portland, OR, USA, Jun./Jul. 2010, pp. 1–7. [Online]. Available: https://ams.confex.com/ams/13CldPhy13AtRad/webprogram/Paper171785.html

[28] A. Angal, X. Xiong, A. Wu, X. Geng, and H. Chen, "Improvements in the on-orbit response versus scan angle characterization of the Aqua MODIS reflective solar bands," *IEEE Trans. Geosci. Remote Sens.*, vol. 56, no. 3, pp. 1728–1738, Mar. 2018.

[29] MODIS Characterization Support Team. (Oct. 21, 2017). *Level-1B (L1B) Calibration Collection 6.0 and Collection 6.1 Changes MODIS Data Alert*. [Online]. Available: https://modis-atmosphere.gsfc.nasa.gov/sites/default/files/ModAtmo/C061_L1B_Combined_v8.pdf

Sunny Sun-Mack received the B.S. degree in astrophysics from Peking University, Beijing, China, the M.S. degree in physics from the University of Maryland, College Park, MD, USA, and the Ph.D. degree in physics from the Tri-Universities Meson Facility (TRIUMF), Simon Fraser University, Vancouver Campus, Vancouver, BC, Canada, in 1994.

She held a research position at the Canada's National Laboratory for Particle and Nuclear Physics, TRIUMF and at the Beijing Astronomical Observatory, China Academia Sinica, Beijing, China. She joined the Clouds and the Earth's Radiant Energy System (CERES) Cloud Working Group, Climate Science Branch, Langley Research Center, National Aeronautics and Space Administration (NASA), Hampton, VA, USA, through various contract companies (Lockheed, SAIC, and, currently, Science Systems and Applications, Inc., Hampton, VA, USA) in 1993. She was involved in many projects, NASA CERES, NPP and JPSS1, and A-Train. Her research interests include clouds and surface remote sensing; validation and integration of cloud properties from Moderate Resolution Imaging Spectroradiometer, Visible Infrared Imaging Radiometer Suite, Cloud-Aerosol Lidar and Infrared Pathfinder Satellite Observation, and CloudSat; and developing and operating large complex end-to-end processing systems.

Patrick Minnis received the B.E. degree in materials science and metallurgical engineering from Vanderbilt University, Nashville, TN, USA, in1972, the M.S. degree in atmospheric science from Colorado State University, Fort Collins, CO, USA, in 1978, and the Ph.D. degree in meteorology from the University of Utah, Salt Lake City, UT, USA, in 1991.

He retired from the Climate Science Branch, Langley Research Center, National Aeronautics and Space Administration (NASA), Hampton, VA, USA, where he served as Senior Research Scientist from 1981 to 2017. He is currently a Consulting Research Scientist with Science Systems and Applications, Inc., Hampton, VA, USA. He supports the NASA Clouds and the Earth's Radiant Energy System and MAP projects and the DOE ARM Program as a part of a research group that also conducts analyses of polar orbiting and geostationary satellite data for field missions, operational aircraft icing condition diagnosis, and contrail research. He has authored or co-authored over 300 peer-reviewed publications. His research interests include remote sensing of clouds and surface properties from satellite imagery for weather and climate investigations.

Dr. Minnis is a Fellow of the American Geophysical Union and American Meteorological Society. He was a recipient of the NASA medals for Exceptional Scientific Achievement in 1993, the Exceptional Achievement in 2005, the Exceptional Service in 2008, the Distinguished Service in 2011, the 2008 AMS Henry G. Houghton Award for Atmospheric Physics, and the 2011 AIAA Losey Atmospheric Sciences Award.

Yan Chen received the B.S. degree in mechanical engineering from Shanghai Jiao Tong University, Shanghai, China in 1984, and the M.S. degree in mechanical engineering from the University of Alabama, Huntsville, AL, USA, in 1992.

Since 2006, she has been with Science Systems and Applications, Inc., Hampton, VA, USA, to support the National Aeronautics and Space Administration (NASA) Clouds and the Earth's Radiant Energy System (CERES), NEWS, and NPP projects. She was with Science Applications International Corporation to support CERES project. She was with CERES Clouds Working Group, NASA, Hampton, VA, USA, where she was involved in satellite data analysis to develop surface emissivity maps, clear sky overhead albedo maps, and algorithm analysis software.

David R. Doelling received the B.S. degree in meteorology from the University of Utah, Salt Lake City, UT, USA, and the M.S. degree in atmospheric science from the University of Washington, Seattle, WA, USA.

He is currently a Senior Research Scientist with the Langley Research Center, National Aeronautics and Space Administration, Hampton, VA, USA, where he is the Time Interpolation and Spatial Averaging Sub-Lead for the Clouds and the Earth's Radiant Energy System (CERES) project and responsible for the diurnal averaging and spatial gridding of CERES footprint cloud and radiative flux parameters. He is also a member of the Geostationary Earth Radiation Budget Experiment and Megha-Tropique Science Teams, projects similar to CERES that measure broadband fluxes. He is currently the Visible Calibration Lead for the Global Space-based Inter-Calibration System, an international effort to improve and harmonize calibration efforts. His research interests include geostationary imager calibration, diurnal averaging techniques of satellite observations, and satellite sampling studies.

Benjamin R. Scarino received the B.S. and M.S. degrees in meteorology from Pennsylvania State University, University Park, PA, USA, in 2008 and 2010, respectively.

He is currently a Senior Research Scientist with Science Systems and Applications, Inc., Hampton, VA, USA, where he supports the work performed with the Langley Research Center, National Aeronautics and Space Administration, Hampton, VA, USA. Specifically, he supports the improvement of the Clouds and the Earth's Radiant Energy System global multispectral cloud and surface property retrieval algorithms, and satellite calibration/radiation property data set development projects. He is a Specialist on intercalibration and trend analysis techniques for geostationary and polar orbiting satellite instruments, developing signal correction algorithms for interinstrument spectral band differences using hyperspectral detectors, and developing absolute calibrations for satellite sensors. He also has specialized skill in using satellite instrument retrievals to derive global high-resolution clear-sky surface skin temperature for use in data assimilation and the earth radiation budget analysis.

Conor O. Haney received the B.S. and M.S. degrees in atmospheric sciences from the University of Illinois at Urbana–Champaign, Champaign, IL, USA, in 2010 and 2013, respectively.

He is currently a Research Scientist with Science Systems and Applications, Inc., Hampton, VA, USA, supporting the contracts of the Langley Research Center, National Aeronautics and Space Administration, Hampton, VA, USA. He is primarily responsible for maintaining the real-time visible sensor calibration for geostationary satellites for the Clouds and Earth's Radiant Energy System project. He is currently developing and improving geostationary visible imager calibration techniques and monitoring their performance.

William L. Smith, Jr. was born in Madison, WI, USA. He received the B.S. degree in meteorology and the Ph.D. degree in atmospheric and oceanic sciences from the University of Wisconsin–Madison, Madison, WI, USA, in 1986 and 2014, respectively, the M.S. degree in atmospheric science from Colorado State University, Fort Collins, CO, USA, in 1989.

He is currently a Research Scientist with the Climate Sciences Branch, Langley Research Center, National Aeronautics and Space Administration (NASA), Hampton, VA, USA, where he has served for 18 years. He leads a research group conducting satellite analyses of clouds and surface properties for weather forecasting, aviation safety, and climate studies. He has lead two major airborne science field campaigns for NASA; The Chesapeake Lighthouse and Aircraft Measurements for Satellites conducted in 2001 and the Arctic Radiation-IceBridge Sea and Ice Experiment conducted in 2014. His research interests include developing physical understandings of clouds and their effects on weather and climate.

Dr. Smith is a member of the American Geophysical Union, American Meteorological Society, and the NASA Clouds and the Earth's Radiant Energy System (CERES) Science Team. He serves as the Chair of the CERES Cloud Retrieval Working Group.